

Surface segregation and ordering of alloy surfaces in the presence of adsorbates

B. C. Han,¹ A. Van der Ven,² G. Ceder,^{1,*} and Bing-Joe Hwang³

¹*Department of Materials Science and Engineering, Massachusetts Institute of Technology, 77 Massachusetts Avenue, Cambridge, Massachusetts 02139, USA*

²*Department of Materials Science and Engineering, University of Michigan, Ann Arbor, Michigan 48109–2136, USA*

³*Nano Electrochemistry Laboratory, Department of Chemical Engineering, National Taiwan University of Science and Technology, Taipei 106, Taiwan, Republic of China*

(Received 15 February 2005; revised manuscript received 21 July 2005; published 7 November 2005)

We argue that surface segregation can be substantially modified by the presence of adsorbates and present a first-principles method that allows us to equilibrate segregation and adsorption simultaneously on surfaces with fixed topology. The method is based on a cluster expansion theory to write the state of the system in terms of adsorbate and surface layer occupation variables. This model can be parametrized with density functional theory calculations and equilibrated at finite temperature with Monte Carlo simulation. The method is applied to surface ordering and segregation at a (111) surface of $\text{Pt}_{(1-x)}\text{Ru}_x$ alloys in the presence of adsorbing oxygen. While Pt segregates under vacuum conditions, the strong binding between oxygen and Ru couples the segregation energy of the Ru to the oxygen chemical potential. As a result, we find that variations in oxygen chemical potential can dramatically alter the segregation and surface ordering tendency of dilute Ru in Pt.

DOI: [10.1103/PhysRevB.72.205409](https://doi.org/10.1103/PhysRevB.72.205409)

PACS number(s): 68.35.Md, 31.15.Ew, 31.15.Ar, 31.15.Dv

I. INTRODUCTION

Inorganic surfaces play a key role in the kinetics of many processes through catalysis of chemical reactions, or as preferred nucleation sites for phase transformations. A crucial step to understanding the mechanism by which such reactions proceed is therefore the detailed chemical and structural characterization of surfaces. Most first-principles calculations are performed under vacuum conditions and provide detailed electronic and structural information. While such calculations can be compared to UHV experiments, they may be less relevant to the understanding of the behavior of a surface in operating environments. In this paper, we develop a method to deal with one particular aspect of nonvacuum conditions, namely, adsorbate controlled surface segregation.

The basic motivation for this work is that the segregation energy of elements in an alloy is influenced by their interaction with the adsorbed layer: when species are adsorbed on the surface, the segregating atoms see a different environment, which will affect their segregation energy. We focus here on segregation to a surface of Pt-Ru alloys important for the catalysis of methanol under varying degrees of oxygen adsorption, though the formalism is independent of this specific chemistry and could be used to study other alloys/adsorbant combinations. Pt catalysts are often alloyed with transition metals in order to enhance their tolerance to carbon mono-oxide (CO) poisoning. For example, addition of Ru to Pt catalysts has been shown to dramatically reduce CO poisoning. While the precise mechanism by which Ru prevents CO poisoning is unclear, it has been proposed that Ru alloying either reduces the bond strength between CO and Pt through its modification of the electronic structure at the catalyst surface^{1,2} or enhances the oxidation of CO to CO_2 by offering a source of oxygen atoms.^{3,4} Both effects would be strongly affected by the arrangement of Ru and Pt on the surface and hence some ability to quantitatively model

segregation under nonvacuum conditions can be useful to optimize catalyst activity and CO tolerance. Figure 1 shows that oxygen adsorption has a profound effect on the segregation of dilute Ru in Pt. It shows the variation of the energy of a nine-layer Pt slab [(111) plane with a 3×3 surface unit cell] as a Ru is brought from the center of the slab (where the energy is set to zero) to layers successively closer to a surface in vacuum [Fig. 1(a)] or with a monolayer of oxygen adsorbed on the surface [Fig. 1(b)]. The methodology to compute the energies is discussed in the next section. Oxygen adsorption turns the positive segregation energy for Ru in a vacuum environment (~ 600 meV),⁵ into a very negative segregation energy (~ -2000 meV). While these calculations correspond to extreme conditions, they clearly demonstrate that the environment present during the processing of a material can play a crucial role in the segregation of alloying elements.

II. MODELS AND METHODS

To study less extreme environments than vacuum or full oxygen coverage, and to investigate in more detail the inter-

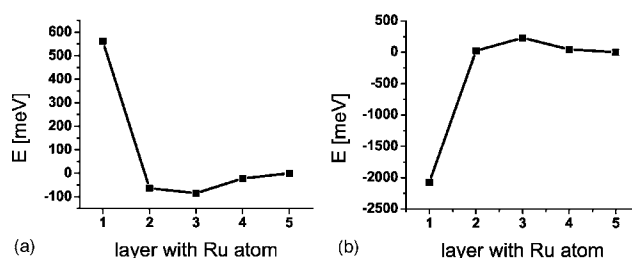


FIG. 1. First-principles energy of a nine-layer (3×3) Pt slab with one Pt atom replaced by a Ru atom. The zero of energy is Ru in the center of the slab (layer 5). (a) in a vacuum (b) with a monolayer oxygen adsorption.

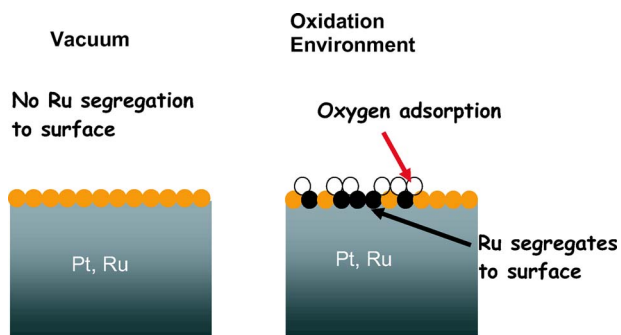


FIG. 2. (Color online) Surface model of the adsorbate and alloy catalyst system.

action between adsorption and segregation we develop a model to predict from first-principles the surface thermodynamics and segregation of an alloy surface as a function of adsorbate chemistry and temperature. This model combines density functional theory (DFT) total energy calculations with a cluster expansion formalism and Monte Carlo simulations to obtain thermally equilibrated surface structures.

Our model consists of three subsystems in contact with each other (Fig. 2). The Pt-Ru alloy is modeled as a surface monolayer on top of bulk which acts as a reservoir with constant chemical potential of Pt and Ru. Each site in this monolayer can be occupied by a Pt or Ru atom. On top of this is a single layer of sites on which adsorbate atoms (oxygen in our case) can be present or not. The adsorbate layer is in chemical equilibrium with an external environment at constant chemical potential of the adsorbate species. The adsorbate layer, surface layer, and the bulk all interact. The restriction of a single alloy surface layer and adsorbate layer in which the configuration is varied is not fundamental to the model and can be easily extended to multiple layers though more interactions in the cluster expansion (see below) would have to be determined. The restriction to a single adsorbate layer obviously restricts application of the model to thermodynamic and kinetic conditions which do not cause adsorbate penetration into the subsurface and bulk (e.g., whole-scale oxidation).

While it is possible to calculate the energy of a few specific arrangements of adsorbates and surface atoms in small unit cells with modern density functional theory methods, chemical equilibrium requires that one samples a large number of configurations, most of which are not periodic. In alloy theory, well established techniques exist to parametrize the energy of a system with respect to configurational occupation variables and then equilibrate it with Monte Carlo simulation.^{6,7} It involves the use of a cluster expansion to extrapolate accurate DFT calculations for a few arrangements of atoms to the calculation of the energy for any arrangement of atoms over a fixed underlying lattice topology. For a material with binary disorder (e.g., a bulk crystalline A - B solution) occupation variables σ_i can be defined which take on the value $+1$ or -1 depending on whether site i is occupied by A or B . A cluster expansion is merely an expansion of the energy of the system in polynomials of these variables:

$$E(\sigma_1, \sigma_2, \dots, \sigma_N) = V_0 + \sum_i V_i \sigma_i + \frac{1}{2} \sum_{i,j} V_{ij} \sigma_i \sigma_j + \frac{1}{6} \sum_{i,j,k} V_{ijk} \sigma_i \sigma_j \sigma_k + \dots \quad (1)$$

These polynomials can be shown to form a complete basis thereby making the untruncated cluster expansion at least formally an exact representation of the energy E .⁶ It may be worth noting that occupation variables σ_i are only needed on sites i for which the occupation is variable, but the energy which is expanded is the *total* energy of the system. Hence, when studying segregation to the surface of an alloy one only needs to expand in the occupation of the first (or first few) layer(s). Since the total energy of the system is expanded, the interaction of these surface layers with the underlying bulk is completely accounted for. This formalism has been used successfully to calculate from first-principles the phase diagrams of a large number of bulk alloys⁷⁻¹¹ and surfaces.^{12,13}

For the Pt-Ru/O surface binary disorder exists both in the alloy surface (Pt or Ru occupation of sites) and in the adsorbate layer (oxygen adsorbed or not) and the results in Fig. 1 indicate that the occupation variables in the adsorbate layer are strongly coupled to the occupation of the underlying surface sites. The energy of such a system with two coupled binary disorder subsystems can in all generality be studied with the coupled cluster expansion.¹⁴ Let the variable $\delta_i = \pm 1$ indicate whether the adsorbate site i is occupied by oxygen or not, and $\sigma_i = \pm 1$ whether the occupation of surface site j is occupied by Pt or Ru. The energy of the system can then be expanded in terms of polynomials of both sets of occupation variables:

$$E(\sigma_1, \sigma_2, \dots, \sigma_N, \delta_1, \delta_2, \dots, \delta_N) = V_0 + \sum_i V_i \sigma_i + \sum_j V_j \delta_j + \sum_{i,j} V_{ij} \sigma_i \sigma_j + \sum_{i,j} V_{ij} \sigma_i \delta_j + \sum_{i,j} V_{ij} \delta_i \delta_j + \dots \quad (2)$$

The expansion contains adsorbate-adsorbate ($\delta_i \delta_j$) interactions, metal-metal ($\sigma_i \sigma_j$) interactions as well as coupling terms ($\sigma_i \delta_j$) between an adsorbate and surface site. Only point and pair terms are shown in Eq. (2), but higher-order polynomials are also considered, and are indeed essential for convergence of the expansion.

While the cluster expansions [Eqs. (1) and (2)] may seem to be simplified models, the completeness of the basis guarantees that the quantity which is expanded can be represented as accurately as one desires. One can think of Eq. (1) as an expansion in the product space of the surface and adsorbate configurational space.¹⁴

Cluster expansions are a useful approach to study the configurational space and finite temperature thermodynamics of systems with fixed topology, i.e., the occupation of the sites can change but their connectivity cannot. Formally, it can be shown that the cluster expansion is an explicit form of the Hamiltonian that is obtained by systematically coarse-graining the partition function of a crystalline system.^{15,16} The results of a such a coarse-graining procedure is a lattice

(or Ising-like) Hamiltonian whose value for a specific configuration gives the free energy obtained by integrating over the non-configurational degree of freedom (e.g., vibrations, electronic excitations). Typically only the ground-state component of their free energy is calculated by placing the atoms on the ideal lattice position and allowing them to locally relax to their lowest energy position. When this ground-state energy is cluster expanded and used in a Monte Carlo simulation to simulate finite temperature behavior, the results only include energy and configurational entropy effects. While for most bulk systems this seems to give high predictive quality and reasonable quantitative agreement with experiment,¹⁷ vibrational effects can be included by expanding the vibrational free energy of each configuration^{18,19} rather than the ground-state configuration. Neglect of vibrations seems to have little effect when studying equilibrium between phases with similar topology²⁰ though it has been shown to be critical to estimate in some cases bulk phase transition between phases with very different topology.²¹

For the adsorption of atomic oxygen^{22–25} we use the fcc hollow sites of a (111) surface, as experimental studies have found these to be more stable than the hcp sites on pure Pt(111).^{26–28} Only the top (111) surface layer of the alloy was given variable occupation so that the adsorbate and surface layer form two coupled triangular lattices on which to perform the coupled cluster expansion.

To parametrize the coupled cluster expansion the energy was calculated for 127 configurations of Pt-Ru in the top layer and oxygen in the adsorbate layer. All configurations fit in a $p(4 \times 4)$ supercell slab of six (111) planes. A vacuum of 14 Å was used in the supercell calculations. The atoms of the top four layers were fully relaxed, while the atoms of the bottom two layers were fixed to their bulk positions. The in-plane lattice parameter was fixed to the calculated lattice parameter of pure Pt and all layers not part of the top surface layers were always pure Pt. Energies were calculated in the generalized gradient approximation (GGA) to density functional theory (DFT) with the Perdew-Wang exchange correlation. The projector augmented wave (PAW) pseudopotentials method was used as implemented in VASP.²⁹ The Kohn-Sham eigenfunctions were expanded in terms of plane waves with a cutoff energy of 250 eV and Brillouin zone integration was performed in on a $21 \times 21 \times 1$ k -point mesh for a (1×1) surface unit cell and on smaller meshes for larger supercells.

While the cluster expansion is formally an exact representation of the energy quantity that is being expanded, its practical value relies on the fact that a truncation limit exists. Which particular polynomials [and therefore which the effective cluster interactions (ECI)] to retain in the expansion were determined by optimizing the cross-validation score of a fit to the calculated DFT energy of the 127 configurations. The cross-validation score is essentially an average measure of how each configuration is predicted when left out of the fit and as such is a measure of the predictive capacity of the expansion.⁹ More details on the cross-validation approach can be found in Ref. 19. Using the cluster expansion equilibrium segregation and adsorption configurations can be obtained by applying Monte Carlo simulations to the cluster expansion (2). We performed the Monte Carlo simulations in

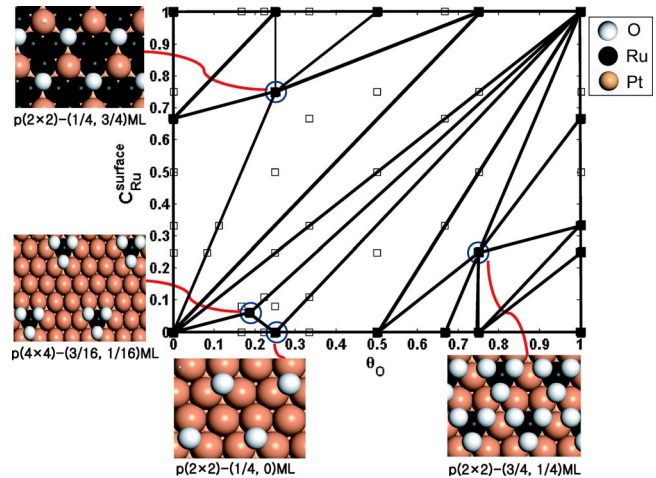


FIG. 3. (Color online) Ground-state structures of the O/Pt-Ru(111) system. The points marked by squares are combinations of oxygen and Ru surface compositions at which the total energy was calculated. The filled squares represent the ground states that make up the convex hull and are stable against decomposition into other structures. Pictures of four of these structures are inserted.

the grand canonical ensemble with an applied oxygen chemical potential (determined by the gas partial pressure) and Ru chemical potential (determined by the bulk concentration of the alloy).

III. RESULTS

A. Stable states of the Pt-Ru | oxygen-vacancy system

Figure 3 shows the surface layer and adsorbate compositions (marked by squares) at which the energies of different configurations were calculated. The solid triangles that connect some of these points are the projection of the convex hull of the 127 energies. The points that define the convex hull (filled squares) are the adsorbate-surface configurations that are stable with respect to linear combinations of arrangements at other compositions that would give the same composition. Hence, the structures corresponding to the filled squares are the groundstates of this adsorbate-surface-layer system. All the other structures (open squares) within a triangle are metastable with respect to the structures at the vertices of that triangle and are able to lower their energy by separating into the structures at the vertices of the triangle in which they lie. The triangles that make up the ground-state map also define all the possible three-phase coexistences at zero K.

The slope of energy with respect to the composition of a species gives the chemical potential of that species. Since each triangle is the projection of a bounding face of the convex energy hull, the slopes of this face are the adsorbate and Ru/Pt chemical potentials that keep the three phases in equilibrium. Most of the groundstate structures are on the edges of the composition diagram and only three exist at intermediate compositions (see inset in Fig. 3). The ground-state map also indicates that pure Pt surfaces partially covered by

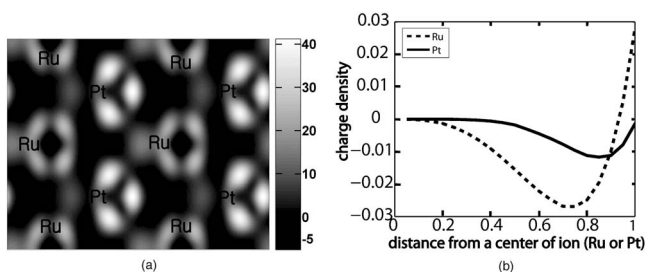


FIG. 4. (a) Difference in charge density of a fully oxidized and fully reduced Ru50%-Pt50% surface (Ru and Pt are arranged in lines). (b) Integral of the charge difference density around Pt (solid line) and Ru (dashed line) as a function of radius of the integration sphere.

oxygen coexists with fully oxygen-covered Ru surfaces, indicating that under equilibrium conditions abrupt oxidation of the surface could occur with minor chemical potential changes of oxygen or Ru. We represent surface structures according to Wood's notation³⁰ and to which we added the oxygen and Ru coverage, i.e., $p(a \times b) - (\theta_1, \theta_2)$ indicates a surface unit cell of dimension a and b with oxygen and Ru surface coverage, respectively, given by θ_1 and θ_2 . A $p(2 \times 2) - (1/4, 0)$ ground-state structure is predicted on pure Pt in agreement with experimental observations using high-resolution electron energy loss spectroscopy (EELS) and LEED (Ref. 31) and with theoretical work.³² While bulk Pt-Ru alloys tend to phase separate in bulk,³³ Fig. 3 shows that in a surface layer exposed to vacuum, ordering between Pt and Ru is favored as evidenced by the stable ordered arrangement at $\theta_{\text{Ru}} = 2/3$. Furthermore, partial oxidation of the surface also tends to stabilize ordered configurations between Pt and Ru within the surface layer (e.g., structure $p(4 \times 4) - (3/16, 1/16)$, structure $p(2 \times 2) - (3/4, 1/4)$ and structure $p(2 \times 2) - (1/4, 3/4)$). As is evident from the inserts showing structure $p(2 \times 2) - (1/4, 3/4)$ and $p(2 \times 2) - (3/4, 1/4)$ there is a strong affinity between oxygen and Ru, with Ru tending to bind oxygen within its nearest-neighbor shell. Hence, we can anticipate that oxygen adsorption will attract bulk Ru to the catalyst surface.

To investigate the strong attraction between oxygen and Ru, we calculated the charge density change when O adsorbs on the surface (Fig. 4). This charge difference plot was obtained by subtracting the charge density of a slab with a particular Pt-Ru arrangement in the surface layer without oxygen coverage from the charge density of the same slab with a monolayer of oxygen on the surface. For this particular purpose no relaxations were allowed so that charge densities could be subtracted point by point. Such a plot therefore illustrates how the charge density changes as a result of oxygen adsorption. The dark regions indicate where oxygen subtracts charge. Figure 4(b) shows the variation with distance of the difference charge density integrated within a sphere around Pt and Ru, respectively. As is clear from both Figs. 4(a) and 4(b), Ru donates more charge to the adsorbed oxygen than Pt consistent with the fact that Ru is more easily oxidized than Pt.

B. Coupled cluster expansion (CCE)

To study the O/Pt-Ru system at finite temperature a coupled cluster expansion was derived from the 127 *ab initio* energies. The optimized cluster expansion contains 40 terms, each corresponding to a cluster of sites (e.g., pair cluster, triplet cluster, etc.), and reproduces the DFT energies with a root mean square (r.m.s.) error of 8 meV per surface site. The cross validation (CV) score of the cluster expansion, which is a measure of its predictive accuracy, is 15 meV. The values of the interaction coefficients (ECIs) are given in Table I along with a figure of each cluster in Fig. 5. The nearest-neighbor pair between an adsorption site and a surface site (cluster 5) is by far the largest interaction. The fact that it is negative reflects the strong attraction between oxygen and Ru (since for oxygen, $\delta = +1$, and for Ru, $\sigma = +1$). The cluster expansion includes pair interactions extending up to the fourth nearest neighbor. Note that several four point clusters (i.e., clusters 57 and 58, see Fig. 5 and Table I) are relatively large, indicating they are essential to the convergence of the cluster expansion. The pure adsorbate terms are positive and decay well with distance, indicating repulsive interactions between oxygens on the surface. The Pt-Ru interactions in the surface layer are all small and positive indicating very weak ordering tendencies in the surface layer.

While it is difficult to make definite statements about the energetics of the system by inspecting the pair ECI, given that there are also triplet and quadruplet ECI present, Table I does give some indication that the structure of this system will be determined by a competition between the adsorbate-adsorbate and adsorbate-surface interaction, with the Pt-Ru interaction in the surface playing a small role.

C. Monte Carlo simulation of finite temperature behavior

The surface structures were thermally equilibrated at fixed Ru and O chemical potential by applying Monte Carlo simulations in a grand canonical ensemble to the coupled cluster expansion. The constant Ru chemical potential condition simulates the bulk acting as infinite reservoir for Ru. While the equilibrium configurations obtained in Monte Carlo simulation are independent of the reference value for the chemical potentials, it is instructive to relate the oxygen chemical potential to an oxygen partial pressure. This can be done through the standard activity equation

$$\mu_{\text{O}}(T, P) = \mu_{\text{O}}^0(T, P^0) + \frac{1}{2}kT \ln\left(\frac{P_{\text{O}_2}}{P^0}\right) \quad (3)$$

In Eq. (3) the oxygen gas is treated as ideal and $\mu_{\text{O}}^0(T, P^0)$ is a reference chemical potential at temperature (T) and pressure (P^0). To find the values for $\mu_{\text{O}}^0(T, P^0)$, we fit our oxygen coverage results for a pure Pt surface to the experimental data at $T = 726$ K obtained by Derry and co-workers³⁴ who measured the oxygen adsorption isotherm for pure Pt as a function of partial pressure and coverage. The reference $\mu_{\text{O}}^0(T, P^0)$ at other temperatures was extrapolated from $T = 726$ K with the analytical free energy function of O_2 gas which includes independent rotational, vibrational and translational degrees of freedom, as for example, given by Hill.³⁵

TABLE I. Effective cluster interaction coefficients (ECIs). (a) The ECI for noncoupled clusters and (b) gives the coupled clusters between adsorbate sites and alloy surface sites. “NN” indicates nearest neighbor.

(a) ECI of noncoupled clusters		
clusters	geometry	interaction (meV)
4	1st NN pair	37.6
8	2nd NN pair	11.1
10	3rd NN pair	4.7
15	4th NN pair	6.2
17	5th NN pair	6.3
3	1st NN pair	4.7
7	2nd NN pair	3.2
11	3rd NN pair	4.5
14	4th NN pair	-0.5
35	triplet	2.0
38	triplet	-1.4
27	triplet	-9.8
36	triplet	2.5
37	triplet	1.6
(b) ECI of coupled clusters		
clusters	geometry	interaction
5	1st NN pair	-152.7
6	2nd NN pair	3.1
9	3rd NN pair	-17.5
12	4th NN pair	-0.3
13	5th NN pair	-4.8
16	6th NN pair	-2.2
31	triplet	-13.8
32	triplet	8.8
33	triplet	-7.0
34	triplet	-4.0
41	triplet	2.4
42	triplet	13.1
45	triplet	-10.5
46	triplet	-7.1
47	triplet	-6.3
50	triplet	-1.9
53	triplet	-1.7
54	triplet	6.8
57	quadruplet	-15.8
58	quadruplet	-11.7
59	quadruplet	4.8
60	quadruplet	-4.5
61	quadruplet	2.2

Table II gives the values of μ_{O}^0 as a function of temperature.

This reference chemical potential contains any energetic offsets between calculation and experiment (either from GGA error or from different choices of reference state) as well as some entropic effects not accounted for in the calcu-

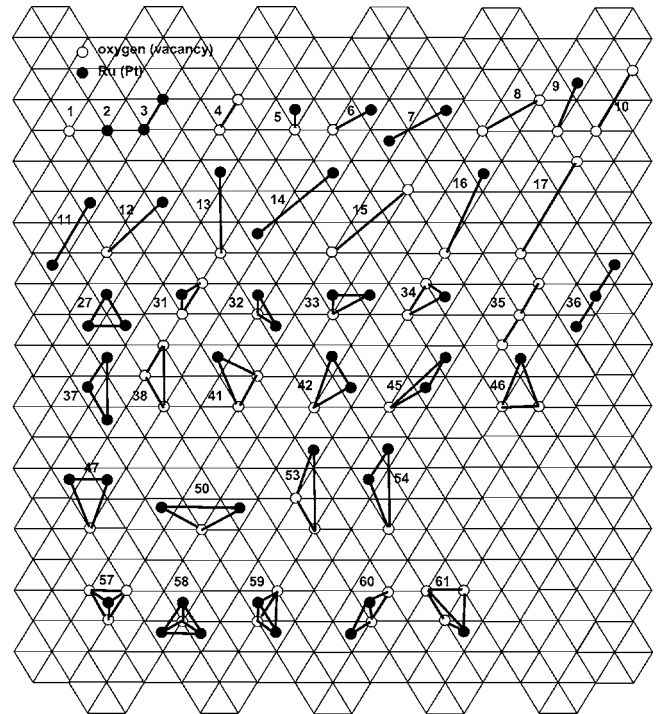


FIG. 5. Effective interactions used in the coupled cluster expansion. The oxygen adsorption sites (open circles) sit on the points of the triangular lattices, while the alloy surface layer sites (solid circles) form another triangular lattice connecting the centers of half the triangles in the figure.

lation. The latter is mainly the entropic loss when oxygen goes from the molecule in the gas to the adsorption site. Note that μ_{O}^0 does not need to fit configurational entropy effects for the adsorbate on the surface as these are explicitly included in the Monte Carlo simulation. Since the non-configurational entropic effects in μ_{O}^0 are dominated by the entropy in the gas phase with some contribution from vibrational entropy on the surface, we believe that it should be

TABLE II. $\mu_{\text{O}}^0(T, P^0)$ at temperature from 100 to 1100 K. These values are obtained from a fit of our Monte Carlo simulation results on pure Pt and oxygen to experimental data at $T=726$ K.³⁴ The values at other temperatures were calculated by the analytical free energy function of a oxygen gas.

T (K)	$\mu_{\text{O}}^0(T, P^0)$ [meV]
100	775.2
200	637.1
300	483.1
400	318.8
500	146.6
600	-32.1
700	-216.3
800	-405.4
900	-598.8
1000	-796.3
1100	-997.3

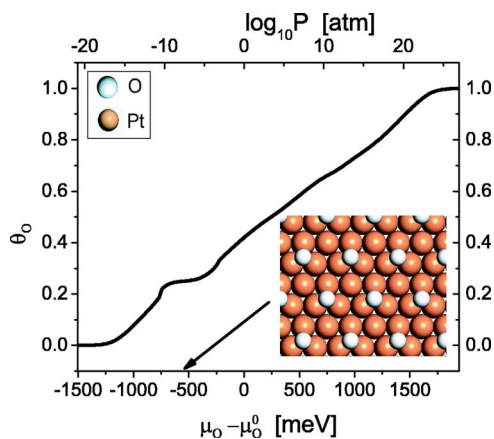


FIG. 6. (Color online) Calculated oxygen coverage on a pure Pt(111) surface at $T=726$ K. The chemical potential (bottom scale) has an arbitrary reference. An approximate oxygen partial pressure (top scale) is given for guidance. The inset shows the stable surface structure at $\theta_O=0.25$.

fairly independent of surface details and therefore transferable from pure Pt surfaces to the Pt-Ru surfaces in our simulation. Fig. 6 shows the oxygen coverage obtained by Monte Carlo simulation as a function of oxygen chemical potential on pure Pt(111) at $T=726$ K. An approximate relation to an oxygen partial pressure scale is made with Eq. (3) and Table II. Our calculation correctly reproduce that at about 10^{-10} – 10^{-5} [atm] adsorbed oxygen orders into a $p(2 \times 2)$ structure (Refs. 31 and 32).

Since the coupled cluster expansion describes the oxygen adsorption energetics and the surface segregation energetics, as well as the interaction between them, it is possible to equilibrate both surface segregation in Pt-Ru and oxygen adsorption simultaneously, and find the true equilibrium states of this system as a function of the chemical potential. Figures 7(a) and 7(b) show equilibrated oxygen isotherms at two different temperatures ($T=600$ and 1050 K) and Ru chemical potentials (-1750 and -665 meV). The horizontal axis corresponds to the oxygen chemical potential and the vertical axis denotes the oxygen concentration (open squares) on the adsorbate lattice and the Ru concentration (filled triangles) in the surface layer. At low Ru chemical potential [Fig. 7(a)], the oxygen concentration only gradually increases, inducing only a slight enhancement of Ru segregation to the surface. As can be seen in the insets, which represent snapshots from the Monte Carlo simulation, the segregated Ru atoms are always bound to adsorbed oxygen atoms. As the oxygen chemical potential increase further, both the oxygen concentration and Ru segregation increase until a full oxygen-covered Ru surface is obtained. Figure 7(b) represents a similar simulation as Fig. 7(a) but at higher Ru chemical potential and at different temperature.

A comparison of Fig. 7(a) with Fig. 7(b) shows that the concentration trajectory changes as the Ru chemical potential increases. At low Ru chemical potential [Fig. 7(a)], the oxygen coverage is always larger than the Ru concentration in the surface layer. But at higher Ru chemical potential (corresponding to a larger Ru bulk concentration), the Ru concentration at the surface exceeds the oxygen concentration

once a threshold oxygen chemical potential is surpassed. Both results [Figs. 7(a) and 7(b)] show that under a high enough oxygen partial pressure, Ru will segregate to the surface. While at low Ru chemical potential [Fig. 7(a)], oxygen adsorption gradually induces Ru segregation, at high Ru chemical potential [Fig. 7(b)], the oxygen adsorption and Ru segregation are strongly coupled, occurring suddenly at a critical oxygen chemical potential. Figures 7(c) and 7(d) show the Monte Carlo simulation results of system 7(a) and 7(b), respectively, at the same temperature and oxygen chemical potential conditions but this time on a pure Pt surface. As is clear from the comparison of Figs. 7(a) and 7(c) or Figs. 7(b) and 7(d), Ru facilitates oxygen adsorption and increases the oxygen coverage dramatically.

The insets in Fig. 7 illustrate that the surface microstructure (ordering between Pt and Ru in the surface layer) changes with temperature and chemical potential. At low oxygen chemical potential, only isolated Ru atoms segregate to the surface. At higher oxygen chemical potential, the Ru atoms that segregate to the surface cluster together, resulting in a surface pattern consisting of islands of Pt surrounded by regions of Ru. At low Ru chemical potential [Fig. 7(a)], the Pt islands are still interconnected, while at higher Ru chemical potential [Fig. 7(b)], the Pt islands are isolated.

IV. DISCUSSION

We have presented an approach to study surface segregation and adsorption simultaneously. By expanding the energy of the system into occupation variables describing the surface and adsorbate sites we can include, without bias, adsorbate-adsorbate, adsorbate-surface, and alloy interactions on the same footing. The advantage of this coupled cluster expansion is that it is formally rigorous since the basis set of expansion functions (the products of the occupation variables) forms a complete set, and its form is independent of the model used to calculate energies of specific surface structures. The choice of clusters and the truncation of the expansion can be optimized through statistical methods such as the cross-validation approach used here,⁹ though other schemes have also been proposed.³⁶ As such the coupled cluster expansion can be a Hamiltonian with all the accuracy of the *ab initio* DFT method by which it is parametrized, but can be evaluated orders of magnitude more faster, making it amenable to Monte Carlo simulation and accurate finite temperature statistics. It is worth pointing out that simpler models in the same spirit, and with the same purpose of studying the interaction between adsorbant and alloy segregation have already been developed.³⁷ One should see our approach as a more formal and generalized extension of these ideas.

In the Pt-Ru system we find a large effect of the adsorbate on the surface segregation in the alloy. While Pt has the lowest surface energy in vacuum and is expect to fully saturate the surface layer at reasonable temperature, the segregation is significantly modified in the presence of oxygen. The strong binding between Ru and O on the surface more than overcomes the higher surface energy of Ru. We find that even at low Ru and oxygen chemical potentials, oxidized

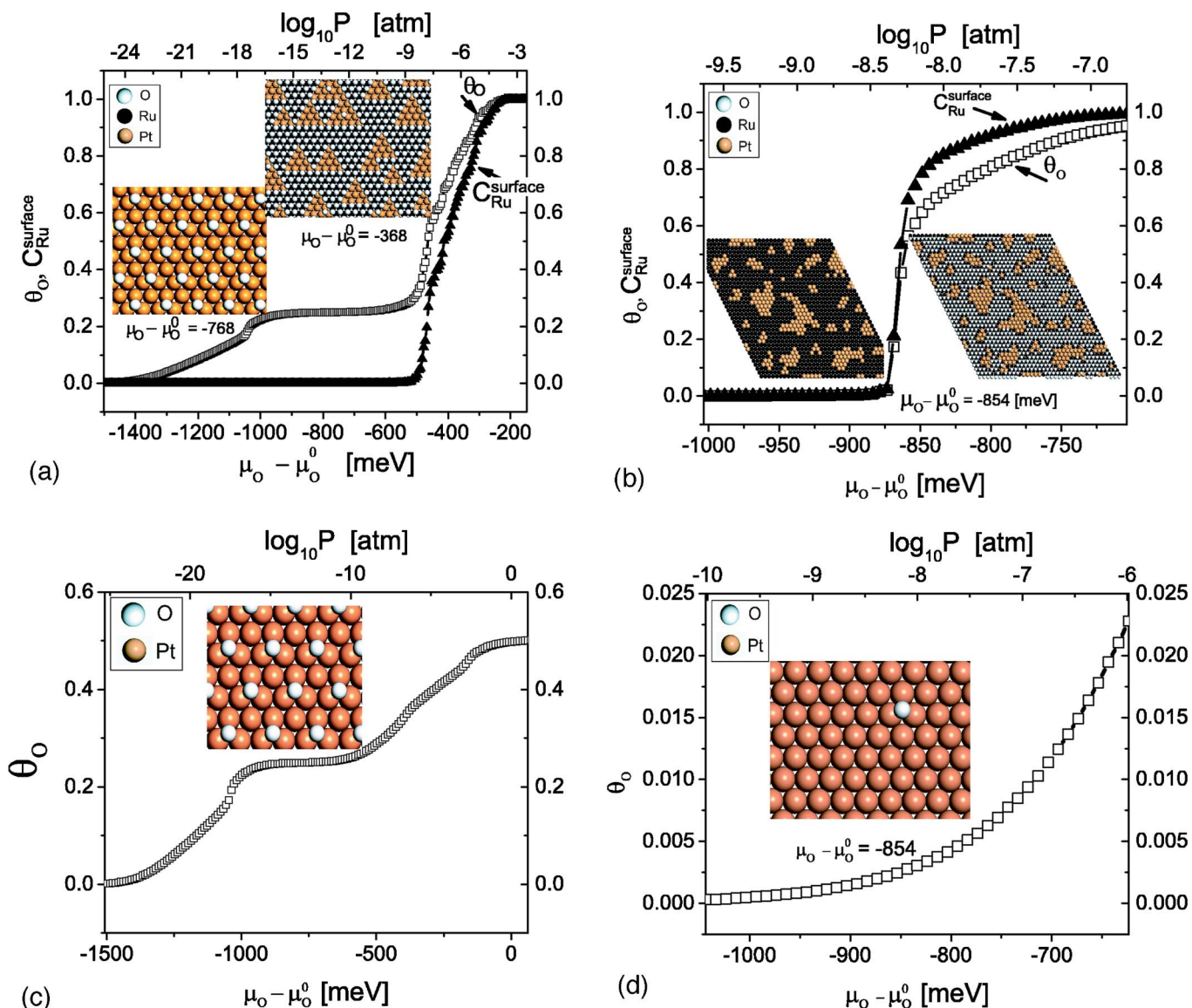


FIG. 7. (Color online) Monte Carlo simulations and surface structure evolutions as a function of oxygen chemical potential μ_O , T and bulk Ru composition C_{Ru} . The conditions of (a) are $T=600$ K, $\mu_{Ru}=-1750$ meV and (b) $T=1050$ K, $\mu_{Ru}=-665$ meV. (c) and (d) are equilibrated oxygen isotherms at $T=600$ K, and $T=1050$ K in pure Pt surfaces with oxygen adsorbates.

islands of Ru coexist with bare Pt on the surface. These island structures are sustained up to very high temperature. At lower temperature and higher Ru chemical potential the combined segregation of Ru to the surface and oxygen adsorption is a collective effect occurring at a critical oxygen chemical potential. Hence, one can think of this as an adsorbate induced segregation transition.

The islands structures that form in our simulation may be important for catalysis as at the edges of the Ru-O islands, both Pt sites for decomposition of methanol and O for the oxidation of CO are available. This is the bi-functional catalyst mechanism which has been proposed in the literature to explain the tolerance of Pt-Ru catalysts to CO.³⁸ If this mechanism is correct, control of the size and structure of the islands would be critical to the catalytic performance of these materials.

Because oxygen adsorption on the surface induces Ru segregation, processing and operating conditions will play an important role in determining the surface structure and composition. Materials formed at temperatures where there is metal atom mobility are likely to have Ru-rich surfaces unless very reducing conditions are used. How this determines the surface of a practical catalyst is unclear as the latter are often washed in mild acids before use, which may remove oxidized species.

In typical fuel cell operation several possible species can adsorb on the catalyst. Using a simpler model Christoffersen *et al.*³⁷ already pointed out that several adsorbed species can induce alloy surface segregation. While typical operating temperatures of fuel cell electrodes are relatively low, it is possible that adsorbant-induced segregation, and subsequent

dissolution of alloying elements contribute to the degradation of catalysts during operation.

On the other hand, surface oxide formation (RuO_2) may also play beneficial roles as it has been shown to enhance particle dispersion of Pt and Ru particle by reducing the degree of sintering during the electrocatalyst manufacturing.³⁹ The dispersion of Pt and Ru in the PtRu electrocatalysts has been proven to be highly essential to their reactivity for methanol oxidation.^{39,40}

Finally, it might be possible to use adsorption induced segregation to pattern surfaces. Our ground state calculations show that ordered structures of $\text{Ru}_{\text{surface}}\text{-O}_{\text{adsorbed}}$ exist for certain ranges of oxygen and Ru chemical potential. These could be formed by long annealing of alloy surfaces under the proper chemical conditions. A short reduction treatment would then remove the surface adsorbant and leave an ordered Ru-Pt surface behind.

When comparing our calculation to experiments several limitations should be kept in mind. We only study the equilibrium states in the (Pt-Ru)-O system and sufficient mobility of Ru through the alloy bulk may be required to allow Ru to diffuse to the surface. Many practical alloy catalysts are prepared through a series of low to medium temperature processes to retain their small particle size, and their surface structure may neither be chemically or structurally equilibrated. In addition, our study focused on a (111) surface, and nanoscale catalysts may have multiple crystallographically different planes.

The other assumption in our work is that adsorbates do not penetrate into the bulk alloy, or Ru does not form a separate oxide phase on the Pt surface. Our model may therefore only be a reasonable approximation in the early stage of oxidation.

Although our methodology was applied to Pt-Ru(111) surfaces in the presence of adsorbed oxygen, it can obviously

be applied to other alloys, adsorbants or surface facets. The important advantage of our coupled cluster expansion is that it offers a general and unbiased approach to study the equilibrium structure in surface-adsorbate problems from first principles. While this makes it possible to calculate surface-adsorbate phase diagrams, the coupled cluster expansion could also be coupled to kinetic Monte Carlo models to study the kinetic evolution of these interesting systems. Such approaches have already been implemented to study diffusion in bulk systems.^{41,42}

V. CONCLUSIONS

We developed and implemented a formalism to study the equilibration of alloy surfaces under a chemical field of adsorbates at finite temperature. Our methodology combines *ab initio* DFT with finite temperature Monte Carlo, connected through the coupled-cluster expansion approach originally developed to study coupled cation/anion disorder in oxides. We applied our methodology to Pt-Ru(111) surfaces and investigated how the surface structures evolve as function of oxygen chemical potential. It is demonstrated that oxygen adsorption can change the surface composition dramatically. Ru is brought to the surface from the bulk by adsorbed oxygen and forms island structures. Hence oxygen can be used as an adsorbate to control the surface morphology during processing of catalysts.

ACKNOWLEDGMENTS

This research was supported by the MURI program of the Army Research Office under Grant No. DAAD19-03-1-0169. Additional support came from NSF (Grant No. ACI-9619020) through computing resources by NPACI at the San Diego Supercomputer Center.

*Corresponding author. FAX: 617-258-6534. Email address: gceder@mit.edu

¹J. McBreen and S. Mukerjee, *J. Electrochem. Soc.* **142**, 3399 (1995).

²M. Watanabe, Y. M. Zhu, H. Igarashi, and H. Uchida, *Electrochemistry (Tokyo, Jpn.)* **68**, 244 (2000).

³H. A. Gasteiger, N. M. Markovic, and P. N. Ross, *J. Phys. Chem.* **99**, 8290 (1995).

⁴T. A. Zawodzinski, T. E. Springer, and S. Gottesfeld, *J. Electrochem. Soc.* **97-2**, 1228 (1997).

⁵E. Christoffersen, P. Liu, A. Ruban, H. L. Skriver, and J. K. Nørskov, *J. Catal.* **199**, 123 (2001).

⁶J. M. Sanchez, F. Ducastelle, and D. Gratias, *Physica A* **128**, 334 (1984).

⁷D. de Fontaine, *Solid State Phys.* **47**, 33 (1994).

⁸A. Zunger, *MRS Bull.* **22**, 20 (1997).

⁹A. Van de Walle and G. Ceder, *J. Phase Equilib.* **23**, 348 (2002).

¹⁰B. P. Burton and A. Van de Walle, *Phys. Chem. Miner.* **30**, 88 (2003).

¹¹M. Asta, V. Ozolins, and C. Woodward, *JOM* **53**, 16 (2001).

¹²B. Sadigh, M. Asta, V. Ozolins, A. K. Schmid, N. C. Bartelt, A. A. Quong, and R. Q. Hwang, *Phys. Rev. Lett.* **83**, 1379 (1999).

¹³O. Wieckhorst, S. Müller, L. Hammer, and K. Heinz, *Phys. Rev. Lett.* **92**, 195503 (2004).

¹⁴P. D. Tapesch, G. D. Garbulsky, and G. Ceder, *Phys. Rev. Lett.* **74**, 2272 (1995).

¹⁵G. Ceder, A. Van der Ven, C. Marianetti, and D. Morgan, *Modell. Simul. Mater. Sci. Eng.* **8**, 311 (2000).

¹⁶G. Ceder, *Comput. Mater. Sci.* **1**, 144 (1993).

¹⁷A. Van der Ven, M. K. Aydinol, and G. Ceder, *Phys. Rev. B* **58**, 2975 (1998).

¹⁸G. D. Garbulsky and G. Ceder, *Phys. Rev. B* **49**, 6327 (1994).

¹⁹A. Van de Walle and G. Ceder, *Rev. Mod. Phys.* **74**, 11 (2002).

²⁰A. Van de Walle and G. Ceder, *Phys. Rev. Lett.* **80**, 4911 (1998).

²¹C. Wolverton and V. Ozolins, *Phys. Rev. Lett.* **86**, 5518 (2000).

²²John L. Gland, Brett A. Sexton, and Galen B. Fisher, *Surf. Sci.* **95**, 587 (1980).

²³N. Materer, U. Starke, A. Barbieri, R. Doll, K. Heinz, M. A. Van Hove, and G. A. Somorjai, *Surf. Sci.* **325**, 207 (1995).

²⁴A. Eichler and J. Hafner, *Phys. Rev. Lett.* **79**, 4481 (1997).

- ²⁵B. C. Stipe, M. A. Rezaei, and W. Ho, *J. Chem. Phys.* **107**, 6443 (1997).
- ²⁶Alexander Bogicevic, Johan Stromquist, and Bengt I. Lundqvist, *Phys. Rev. B* **57**, R4289 (1998).
- ²⁷K. Bleakley and P. Hu, *J. Am. Chem. Soc.* **121**, 7644 (1999).
- ²⁸M. Lynch and P. Hu, *Surf. Sci.* **458**, 1 (2000).
- ²⁹G. Kresse and D. Joubert, *Phys. Rev. B* **59**, 1758 (1999).
- ³⁰E. A. Wood, *J. Appl. Phys.* **35**, 1306 (1964).
- ³¹H. Steininger, S. Lehwald, and H. Ibach, *Surf. Sci.* **123**, 1 (1982).
- ³²Hairong Tang, A. Van der Ven, and Berhardt L. Trout, *Phys. Rev. B* **70**, 045420 (2004).
- ³³J. M. Hutchinson, *Platinum Met. Rev.* **16**, 88 (1972).
- ³⁴G. N. Derry and P. N. Ross, *J. Chem. Phys.* **82**, 2772 (1985).
- ³⁵Terrell L. Hill, *An Introduction to Statistical Thermodynamics*, 2nd ed. (Addison-Wesley, New York, 1962), Chap. 8.
- ³⁶C. L. Mallow, *Technometrics* **15**, 661 (1973).
- ³⁷E. Christofferssen, P. Stoltze, and J. K. Nørskov, *Surf. Sci.* **505**, 200 (2002).
- ³⁸M. Watanabe and S. Moto, *J. Electroanal. Chem. Interfacial Electrochem.* **60**, 267 (1975).
- ³⁹T. R. Ralph and M. P. Hogarth, *Platinum Met. Rev.* **46**, 117 (2002).
- ⁴⁰B.-J. Hwang, L. S. Sarma, J.-M. Chen, C.-H. Chen, S.-C. Shih, G.-R. Wang, D.-G. Liu, J.-F. Lee, and M.-T. Tang, *J. Am. Chem. Soc.* **127**, 11140 (2005).
- ⁴¹A. Van der Ven, G. Ceder, M. Asta, and P. D. Tepesch, *Phys. Rev. B* **64**, 184307 (2001).
- ⁴²A. Van der Ven and G. Ceder, *Phys. Rev. Lett.* **94**, 045901 (2005).